Laminar Flow at a Three-Dimensional Stagnation Point with Large Rates of Injection

Paul A. Libby*
University of California, San Diego, La Jolla, Calif.

Exact calculations of the titled flow are presented and compared to the predictions of an asymptotic analysis for large rates of injection. The inner layer of the boundary layer is found to involve outflow in both orthogonal directions whether the external flow along the y axis is inward or outward. As a result, the flow at a nearly two-dimensional stagnation point involves drastic changes as a weak outflow changes to a weak inflow. It is also found that the velocity profiles in the two directions in the inner layer are quite different.

Nomenclature

a = velocity gradient in x direction du_e/dx
b = velocity gradient in y direction dv_e/dy
c = b/a
f = modified stream function $f'(\eta) = u/u_e$
u,v,w = velocity components in x-, y-, z-direction respectively
x,y,z = cartesian coordinates
g = static enthalpy ratio h/h_e
h = static enthalpy
ϵ = expansion parameter $-(f(0)+c\varphi(0))^{-1}$
Δ_x = momentum thickness in the x-wise boundary layer
Δ_y = momentum thickness in the y-wise boundary layer
Δ^* = displacement thickness
ρ = mass density
μ = coefficient of viscosity
σ = Prandtl number
φ = modified stream function $\varphi'(\eta) = v/v_e$
η = similarity variable, cf. Eq. (1)
$\bar{\eta}$ = inner layer similarity variable
$\hat{\eta}$ = outer layer similarity variable
γ = wall enthalpy parameter $g^{1/2}(0)$
λ_i = coefficients in translational transformation, cf. Eq. (14)

Subscripts

e = value in external stream
w = value at the surface

Introduction

THE laminar boundary layer at a general, three-dimensional stagnation point has received the attention of several investigators.[1-3] Such layers are of fundamental interest because the putative flows at two-dimensional and axisymmetric stagnation points are only special cases of those which arise if the velocity gradients in orthogonal directions in the external stream are arbitrarily related. There is also applied interest in the heating rates which occur at these general stagnation points in high speed flight.

We are concerned here with the boundary-layer characteristics at three-dimensional stagnation points when large rates of injection occur. It is known that under some conditions, either of intense radiative heat transfer or of transpiration cooling, mass is injected into the boundary layer at sufficiently high rates so as to alter significantly the features of the flow from those usually expected. In particular, we know[4-6] that with high rates of injection the boundary layer developes a structure consisting of a thin outer layer adjusting the inner layer to the external flow, and of a relatively thick inner layer wherein inertia and pressure forces are dominant and shear forces negligible.

Libby and Kassoy[6] analyze an example of a three-dimensional boundary layer subject to high rates of injection, specifically that at a swept stagnation line of doubly-infinite extent. In this case the chordwise and spanwise flows within the inner layer respond differently. Accordingly, we consider it of interest to study another three-dimensional case and to learn how the boundary layer at a three dimensional stagnation point is effected by large rates of injection.

After our study was nearly complete, Gersten[7] published results of an analysis of the laminar boundary layer at a three-dimensional stagnation point with intense suction or injection. With respect to injection, the only case considered here, the general approaches followed here and by Gersten are quite similar, but the emphasis and details differ and the results are complementary. In particular, the outer solutions, and the matching of the inner and outer solutions, are presented here so that a detailed discussion of the various profiles can be given.

Generally we confine our attention to the more practical but limited range of c, i.e., to $0 \leq c \leq 1$. It is known[3] that multiple solutions prevail, and therefore that questions of observability arise for $c<0$. However, the case $-1<<c<0$ differs considerably from the case $0<c<<1$ when the injection is large; as a consequence we do comment on the effect of small negative c, i.e., of a weak inflow along the y axis with an outflow along the x axis. In addition, for the case $c=-1$, the inner solutions can be obtained in closed form and are therefore given.

In studying these flows we follow the strategy of Libby and Kassoy,[6] i.e., we carry out the numerical analysis for large rates of injection and develop an approximate asymptotic analysis which permits the numerical results to be extended to indefinitely large rates of injection. The asympototic analysis, although approximate, circumvents the difficulties in numerical analysis which usually become progressively more severe as the injection rate increases. Nachtshein and Green[8] have shown how a method based on integration in two directions from the dividing streamline may be employed to overcome these difficulties.

Analysis

For the purposes of this study it is justified to make certain simplifying assumptions concerning the description of the transport and thermodynamic properties of the gas. Ac-

Received September 15, 1975; revision received November 24, 1975. The research reported here was initially supported by NASA under grant NGR 05-009-190 which expired Jan. 14, 1973. The author gratefully acknowledges the early work of Peter Poulsen on this research and the helpful discussions with William Bush and Lu Ting.

Index category: Bounday Layers and Convective Heat Transfer – Laminar.

*Professor and Chairman, Department of Applied Mechanics and Engineering Sciences. Fellow AIAA.

cordingly, we follow closely Ref. 3 and assume we have a homogeneous gas with a mass density inversely proportional to the static enthalpy $\rho\alpha h^{-1}$; a constant product of mass density and coefficient of viscosity $\rho\mu \simeq \rho_e\mu_e$; and a constant Prandtl number σ. Further analysis removing these assumptions can be reaily performed by the strategy employed here. We follow usual practice and carry out the analysis in terms of a single independent variable η which is related to the physical quantities according to

$$\eta=\left(\frac{\rho_e a}{\mu_e}\right)^{1/2}\int_0^z\left(\frac{\rho}{\rho_e}\right)dz' \tag{1}$$

With these assumptions the boundary layer is described by the solution of the following set of coupled similarity equations[3]

$$f'''(\eta)+(f+c\varphi)f''+(g-f'^2)=0 \tag{2}$$

$$\varphi'''(\eta)+(f+c\varphi)\varphi''+c(g-\varphi'^2)=0 \tag{3}$$

$$g''(\eta)+\sigma(f+c\varphi)g'=0 \tag{4}$$

For clarity it is appropriate to relate here the quantities of physical interest to the variables f, φ, and g; the velocity components are given by

$$u=axf'=u_e f';\quad v=by\varphi'=v_e\varphi';$$

$$w=-(\rho_e/\rho)(v_e a)^{1/2}(f+c\varphi)$$

while $(\rho_e/\rho)=(h/h_e)=g$.

The boundary conditions relative to u, v, and g are obvious; we take

$$f'(0)=\varphi'(0)=0,\quad f'(\infty)=\varphi'(\infty)=g(\infty)=1$$

$$g(0)=g_w\equiv\gamma^2, \text{ given}$$

The conditions at $\eta=0$ relative to w require some comment. In Eqs. (1-3) f and φ appear only in the combination $f+c\varphi$, so that without loss of generality we could take $\varphi=0$ and let $f(0)$ establish the normal velocity as in Ref. 3. However, it will be found convenient below in connection with our asymptotic analysis for large rates of injection to specify only the sum $f(0)+c\varphi(0)$, and to require that at some $\eta=\eta_0$, $f(\eta_0)=\varphi(\eta_0)=0$. At the location corresponding to $\eta=\eta_0$, $w=0$; i.e., the stream surfaces branch and a stagnation point within the boundary layer exists.

It is important to note that a solution corresponding to $f(0)=f_w$, $\varphi(0)=0$ can be converted to one satisfying the conditions we presently desire by adding constants α and β to f and φ respectively, subject to the conditions $\alpha+c\beta=0$ and $f(\eta_0)+\alpha=\varphi(\eta_0)+\beta=0$.

Quantities of Technical Interest

From the numerical solutions of the above equations the quantities of technical interest are the heat transfer related directly to $g'(0)\equiv g'_w$, and the skin-friction coefficients related to $f''(0)\equiv f''_w$, $\varphi''(0)\equiv\varphi''_w$. In addition certain integral thicknesses which characterize the integral properties of the boundary layer are related directly to

$$\Delta_x\equiv\int_0^\infty f'(1-f')\,d\eta$$

$$\Delta_y\equiv\int_0^\infty \varphi'(1-\varphi'(1-\varphi')\,d\eta$$

$$\Delta^*\equiv\int_0^\infty[g-(f'+c\varphi')(1+c)^{-1}]d\eta \tag{5}$$

Accordingly, the results of our numerical analysis will be presented in terms of these quantities, of η_0, and of the crucial wall values required to reproduce the complete solutions with a single integration; namely $f(0)$, $\varphi(0)$, $f''(0)$, $\varphi''(0)$, $g'(0)$.

Asympototic Analysis – Inner Solution

We develop next an approximate analysis for large $-\rho w$. Consider a small parameter $\epsilon\equiv-[f(0)+c\varphi(0)]^{-1}$. The anticipated development of a thick inner layer and relatively thin outer layer as discussed earlier, suggests rescaling of the independent and dependent variables. After Libby and Kassoy,[6] we let $\tilde\eta\equiv\epsilon\eta$, $\tilde f\equiv\epsilon f$, $\tilde\varphi\equiv\epsilon\varphi$, $\tilde g\equiv g$. In terms of these new variables, Eqs. (2-4) become without further approximation

$$\epsilon^2\tilde f'''(\tilde\eta)+(\tilde f+c\tilde\varphi)\tilde f''+(\tilde g-\tilde f'^2)=0 \tag{6}$$

$$\epsilon^2\tilde\varphi'''(\tilde\eta)+(\tilde f+c\tilde\varphi)\tilde\eta''+c(\tilde g-\tilde\varphi'^2)=0 \tag{7}$$

$$\epsilon^2\tilde g''(\tilde\eta)+\sigma(\tilde f+c\tilde\varphi)\tilde g'=0 \tag{8}$$

The boundary conditions are

$$\tilde f(\tilde\eta=0)+c\tilde\varphi(\tilde\eta=0)=-1,\quad \tilde f'(\tilde\eta=0)=\tilde\varphi'(\tilde\eta=0)=0,$$

$$\tilde g(\tilde\eta=0)=g_w\equiv\gamma^2,\quad \tilde f'(\tilde\eta\to\infty)=\tilde\varphi'(\tilde\eta\to\infty)=\tilde g(\tilde\eta\to\infty)=1,$$

and

$$\tilde f(\tilde\eta=\tilde\eta_0)=\tilde\varphi(\tilde\eta=\tilde\eta_0)=0$$

Although these equations are exact, their main value lies in their provision of a basis for systematic approximations through a power series in ϵ for $\epsilon\ll1$. Suppose $\tilde f$, $\tilde\varphi$, $\tilde g$ are represented by such a series with the first terms denoted by $\tilde f_0$, $\tilde\varphi_0$, $\tilde g_0$; then

$$(\tilde f_0+c\tilde\varphi_0)\tilde f_0''(\tilde\eta)+(\tilde g_0-\tilde f_0'^2)=0 \tag{9}$$

$$(\tilde f_0+c\tilde\varphi_0)\tilde\varphi_0''(\tilde\eta)+c(\tilde g_0-\tilde\varphi_o'^2)=0 \tag{10}$$

$$(\tilde f_0+c\tilde\varphi_0)\tilde g_0'(\tilde\eta)=0 \tag{11}$$

provided $\tilde f_0+c\tilde\varphi_0\neq0$. This condition defines the outer edge of the inner layer identified by $\tilde\eta=\tilde\eta_0$, and we seek solutions for $0\le\tilde\eta\le\tilde\eta_0$. Matching requirements necessitate that at this edge $\tilde f_0(\tilde\eta_0)=\tilde\varphi_0(\tilde\eta_0)=0$; these conditions have the consequence that $\tilde\eta_0$ is an approximation to η_0, with errors of 0(1) compared to ϵ^{-1}. Inspection of these equations also suggest that the case $c=0$ is special since $\tilde\varphi_0(\eta)\equiv0$; this case will be treated later.

Eqs. (9) and (10) with $\tilde g_0\equiv\gamma^2$ are to be solved subject to the conditions

$$\tilde f_0(0)+c\tilde\varphi_0(0)=-1,\quad \tilde f_0'(0)=\tilde\varphi_0(0)=0$$

$$\tilde f_0(\tilde\eta_0)=\tilde\varphi_0(\tilde\eta_0)=0 \tag{12}$$

We now draw some consequences from Eqs. (9)-(12) prior to their actual solution. First we note that the inner layer solutions are independent of the Prandtl number. Next $\tilde f_0''(\tilde\eta=0)=\gamma^2$, $\tilde\varphi_0''(\tilde\eta=0)=c\gamma^2$. While we shall need a more detailed consideration of the behaviour of $\tilde f_0$ and $\tilde\varphi_0$ near $\tilde\eta=\tilde\eta_0$, for immediate purposes we note that $\tilde f_0'(\tilde\eta=\tilde\eta_0)=\gamma$; that for $c>0$, $\tilde\varphi'(\tilde\eta=\tilde\eta_0)=\gamma$; and that for $c<0$, $\tilde\varphi'(\tilde\eta=\tilde\eta_0)=-\gamma$.

This last result is a special case of the general feature that $\tilde f_0(\tilde\eta;c)=\tilde f_0(\tilde\eta;-c)$, $\tilde\varphi_0(\tilde\eta;c)=-\tilde\varphi_0(\tilde\eta;-c)$. The physical implication of this behavior is as follows: for $c>0$ there is outflow from the stagnation point in all directions and in both the inner and external flows; for $c<0$ there is outflow

throughout the inner layer and along the x axis in the external flow, but in-flow in the external flow along the y axis associated with $c<0$. Thus the mass transfer causes outflow in the inner layer despite the external pressure gradient. Clearly a severe adjustment of the inner layer and external flow is required in the case of $c<0$.

Consider next additional terms in ϵ derivable from Eqs. (6-8); the solutions for $\tilde{g}_i$, $i=1$, ... are identically zero; i.e., $\tilde{g}(\tilde{\eta})=\gamma^2$ to all orders in ϵ. The equations for $\tilde{f}_1(\tilde{\eta})$, $\tilde{\varphi}_1(\tilde{\eta})$, etc., will be inhomogeneous equations subject to homogeneous boundary conditions

$$\tilde{f}_i(\tilde{\eta}=0)+c\tilde{\varphi}_i(\tilde{\eta}=0)=0, \quad \tilde{f}_i'(\tilde{\eta}=0)=\tilde{\varphi}_i'(\tilde{\eta}=0)$$

$$=\tilde{f}_i(\tilde{\eta}=\tilde{\eta}_0)+\tilde{\varphi}_i(\tilde{\eta}=\tilde{\eta}_0)=0, \quad i=1,2,\ldots$$

A consideration of the consequent behavior at $\tilde{\eta}=0$ is that $\tilde{f}_i''(\tilde{\eta}=0)=\tilde{\varphi}_i''(\tilde{\eta}=0)=0$, $i=1,2$, ...; thus the values of $\tilde{f}_0''(\tilde{\eta}=0)$ and $\tilde{\varphi}_0''(\tilde{\eta}=0)$ provide the only estimate for the wall shear parameters, namely $f''(\eta=0)=\epsilon\gamma^2$, $\varphi''(\eta=0)=\epsilon\gamma^2$.

We now consider in more detail the behavior of the inner solutions near $\tilde{\eta}=\tilde{\eta}_0$, since that behavior determines the outer solutions; from Eqs. (6) and (7) it is easy to find that for $\tilde{\eta}\leq\tilde{\eta}_0$,

$$\tilde{f}_0(\tilde{\eta})\cong-\gamma(\tilde{\eta}_0-\tilde{\eta})+A_m(\tilde{\eta}_0-\tilde{\eta})^{1+m}+\ldots$$

$$\tilde{\varphi}_0(\tilde{\eta})\cong-\gamma(\tilde{\eta}_0-\tilde{\eta})+B_n(\tilde{\eta}_0-\tilde{\eta})^{1+n}+\ldots \tag{13}$$

where for $0<c<1$, $0<n<1<m<2$, $n\equiv 2c/(1+c)$, $m\equiv 2/(1+c)$; thus there is a distinct difference in the second derivatives of $\tilde{f}_0$ and $\tilde{\varphi}_0$ near $\tilde{\eta}=\tilde{\eta}_0$, a difference which enters into the treatment of the outer solution. We sketch the implications of Eqs. (13) in Fig. 1; qualitatively, $\tilde{f}_0'(\tilde{\eta})$ behaves the same way for any $0<|c|<1$ and approaches its value γ as $\tilde{\eta}\to\tilde{\eta}_0$ with zero slope. On the contrary the y-wise profile $\tilde{\varphi}_0'(\tilde{\eta})$ has an infinite slope at $\tilde{\eta}=\tilde{\eta}_0$ for $c\neq\pm 1$. Note that this behavior is independent of γ, i.e., it does not depend on differences in density in the inner and outer flows, but occurs for the case $\gamma=1$ as well. Note further that for $-1<c<0$ the sign of $\tilde{\varphi}_0$ must be changed. As a consequence, for this range of c, the definitions of the exponents n and m involve c replaced by $|c|$. The coefficients A_m and B_n can be determined from the solution for $\tilde{f}_0(\tilde{\eta})$ and $\tilde{\varphi}_0(\tilde{\eta})$.

It appears that in general, numerical analysis is required to obtain solutions to Eqs. (6) and (7), which now depend only on two parameters, c and γ^2. However, for the limiting cases $c=\pm 1$, we know[3,4] that simple analytical solutions exist; namely

$$\tilde{f}_0=c\tilde{\varphi}_0=-\tfrac{1}{2}+\gamma^2/2\tilde{\eta}^2, \quad \tilde{\eta}_0=\gamma-1$$

which gives

$$\tilde{f}_0'(\tilde{\eta})=\gamma^2\tilde{\eta}, \quad \tilde{f}_0''(\tilde{\eta})=\gamma^2$$

In addition, if $c=0$, then $\tilde{\varphi}_0\equiv 0$ and we have an analytic solution for $\tilde{f}_0$, namely

$$\tilde{f}_0=-\cos\gamma\tilde{\eta}, \quad \tilde{\eta}_0=(\pi/2)\gamma^{-1}$$

which gives

$$\tilde{f}_0'(\tilde{\eta})=\gamma\sin\gamma\tilde{\eta}, \quad \tilde{f}''(\tilde{\eta})=\gamma^2\cos\gamma\tilde{\eta}$$

Thus the case $c=0$, excluded earlier, poses no special difficulties per se, but the drastic difference in the behavior for $c^2\ll 1$, $c>0$ and $c<$ indicates that the cases $c=0^+$, 0^- are significantly different.

Asymptotic Analysis – Outer Solutions

The outer solutions involve a thin layer which is removed from the surface by the injection; thus a translated but unstretched coordinate, denoted $\hat{\eta}$, is indicated. The origin of the $\hat{\eta}$ coordinate relative to η is somewhat uncertain and depends on a series in ϵ. In particular we let

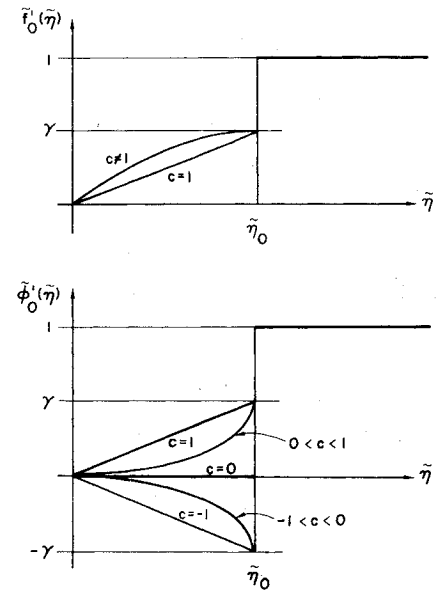

Fig. 1 Schematic representation of the velocity distributions in the inner layers, injection parameters $\gamma^2=0.1$; −, prediction of asymptotic analysis.

$$\hat{\eta}=\eta-\tilde{\eta}_0/\epsilon-\lambda_1-\epsilon\lambda_2+\ldots \tag{14}$$

where λ_i are constants to be determined in the course of the analysis. Although we shall specify boundary conditions at $\hat{\eta}=0$, the value of η corresponding to $\hat{\eta}=0$ for a given ϵ will depend on the number of terms included in Eq. (14).

Because the outer layer is thin, the values of f, φ, and g in the outer layer are unscaled but for clarity are denoted as $\hat{f}$, $\hat{\varphi}$, and $\hat{g}$. The equations therefor are Eqs. (2-4) with η, f, φ, and g replaced by $\hat{\eta}$, $\hat{f}$, $\hat{\varphi}$, and $\hat{g}$. Continuing with the idea of an approximate asymptotic solution, we consider series solutions in terms of appropriate powers of ϵ. Various considerations, especially those reflecting matching with the inner solutions near $\tilde{\eta}\leq\tilde{\eta}_0$ as given by Eq. (13), suggest

$$\hat{f}(\hat{\eta};\epsilon)=\hat{f}_0(\hat{\eta})+\epsilon\hat{f}_1(\hat{\eta})+\epsilon^m\hat{f}_m(\hat{\eta})+\ldots$$

$$\hat{\varphi}(\hat{\eta};\epsilon)=\hat{\varphi}_0(\hat{\eta})+\epsilon^n\hat{\varphi}_1(\hat{\eta})+\ldots$$

$$\hat{g}(\hat{\eta};\epsilon)=\hat{g}_0(\hat{\eta}) \tag{15}$$

It is illuminating to consider these expansions for limiting and special cases of c; for $c=\pm 1$, $m=n=1$ and the second term in the representation of $\hat{f}(\hat{\eta})$ and $\hat{\varphi}(\hat{\eta})$ will be proportional to ϵ. In this case $\hat{f}_1(\hat{\eta})$ and $\hat{\varphi}_1(\hat{\eta})$ will remove the discontinuity in $\tilde{f}''(\tilde{\eta})=\tilde{\varphi}''(\tilde{\eta})$ $\tilde{\eta}=\tilde{\eta}_0$. For $c=0$, $n=0$ and the second term in each series is again proportional to ϵ, denoted $\hat{f}_1(\hat{\eta})$, $\hat{\varphi}_1(\hat{\eta})$ in Eqs. (15); however $\hat{\varphi}_n(\hat{\eta})$ will be found useful in this case. For general c it should be noted that $\hat{\varphi}_n(\hat{\eta})$ compensates for the unpleasant behavior of $\tilde{\varphi}_0(\tilde{\eta})$ near $\tilde{\eta}\leq\tilde{\eta}_0$ noted earlier (cf. Fig. 1).

The equations for $\hat{f}_0$, $\hat{\varphi}_0$, and $\hat{g}_0$ are actually Eq. (2-4), with the previously described replacement of variables. We discuss first cases where $c\neq 0$. The appropriate boundary conditions are

$$\hat{f}_0'(\hat{\eta}\to\infty)=\hat{\varphi}_0'(\hat{\eta}\to\infty)=\hat{g}_0(\hat{\eta}\to\infty)=1$$

$$\hat{f}_0(\hat{\eta}=0)+c\hat{\varphi}_0(\hat{\eta}=0)=0 \tag{16}$$

With Eqs (13) written in terms of the outer variables, the usual matching procedure results in the additional conditions

$$\lim_{\hat{\eta}\to\infty}(\hat{f_0}(\hat{\eta})+\gamma(-\hat{\eta}-\lambda_1))=0$$

$$\lim_{\hat{\eta}\to\infty}(\hat{\varphi}_0(\hat{u})+\mathrm{sgn}(c)\gamma(-\hat{\eta}-\lambda_1))=0$$

$$\lim_{\hat{\eta}\to\infty}(\hat{g}_0(\hat{\eta})-\gamma^2)=0 \qquad (17)$$

A unique value for λ_1 is assured if one of the first two equations is replaced by

$$\lim_{\hat{\eta}\to\infty}(\hat{\varphi}_0(\hat{\eta})+\mathrm{sgn}(c)\gamma(-\hat{\eta}-\lambda_1))=0$$

The equation for $\hat{\varphi}_n(\hat{\eta})$ is found from Eqs. (2-4), with the variables replaced as discussed previously and the series given by Eqs. (15) substituted; collecting the ϵ^n terms, we obtain

$$\hat{\varphi}_n'''(\hat{\eta})+(\hat{f_0}+c\hat{\varphi}_0)\hat{\varphi}_n''+c\hat{\varphi}_0'\hat{\varphi}_n-2c\hat{\varphi}_0'\hat{\varphi}_n'=0 \qquad (18)$$

One obvious boundary condition is $\hat{\varphi}_n'(\hat{\eta}\to\infty)=0$; the other two arise from matching with $\bar{\varphi}_0(\bar{\eta})$. Equation (13) gives the condition

$$\lim_{\hat{\eta}\to-\infty}(\hat{\varphi}_n(\hat{\eta})-\mathrm{sgn}(c)B_n(-\hat{\eta}-\lambda_1)^{1+n})=0 \qquad (19)$$

where B_n and λ_1 are known from $\bar{\varphi}_0(\bar{\eta})$. To see if $\hat{\varphi}_n$can behave in the requisite fashion for large negative $\hat{\eta}$, we must consider the asymptotic behavior of Eq. (18); we find for large $-\hat{\eta}$

$$\hat{\varphi}_n'(\hat{\eta})\sim Ce^{-\frac{1}{2}(1+|c|)\gamma\hat{\eta}^2}(-\hat{\eta})^{n-1}+D(-\hat{\eta})^n \qquad (20)$$

where $n=2|c|/(1+|c|)$. Accordingly, if we supress the exponential terms, we can obtain the desired asymptotic behavior of $\hat{\varphi}_n(\hat{\eta})$; we thus supplement Eq. (19) with the condition which assures that appropriate power law behavior, namely

$$\lim_{\hat{\eta}\to-\infty}\left(\hat{\varphi}_n'(\hat{\eta})+\frac{(1+n)\hat{\varphi}_n(\hat{\eta})}{(-\hat{\eta}-\lambda_1)}\right)=0 \qquad (21)$$

Equations (19) and (20), plus the condition at $\eta\to\infty$, determine $\hat{\varphi}_n(\hat{\eta})$.

Consider now the case $c=0$. The appearance throughout the preceding analysis of sgn(c) in $\hat{\varphi}_0(\eta)$ and $\hat{\varphi}_n(\eta)$ suggests that $c=0$ is special for the y-wise velocity distribution. In fact the previous analysis is unaltered for $\hat{f_0}(\eta)$ if $c=0$. However, for $c=0$, $\hat{\varphi}(\eta)$ to lowest order in ϵ is strictly given by the linear equation $\hat{\varphi}'''(\hat{\eta})+f_0\hat{\varphi}''=0$ which is to be solved subject to the boundary conditions

$$\hat{\varphi}'(\hat{\eta}\to\infty)=1, \qquad \lim_{\hat{\eta}\to-\infty}\hat{\varphi}(\hat{\eta})=0$$

If this solution is sought, we recognize discontinuous behavior as $c^2\sim 0$, i.e., as $\hat{\eta}\to-\infty$ for $c=0^+$, 0^-, $\hat{\varphi}\sim\mathrm{sgn}(c)\gamma(-\hat{\eta}-\lambda_1)$ compared to $\hat{\varphi}\sim 0$ for $c=0$. However, we notice that for $c=0$, $n=0$ and for the second of Eqs. (15) we can consider that the combination $\hat{\varphi}_0+\hat{\varphi}_n$ gives this lowest order solution. From this point of view it is convenient to compute $\hat{\varphi}_0(\hat{\eta};\ c=0^+,\ 0^-)$.

The next terms in the outer solutions, $\hat{f_1}(\hat{\eta})$ and $\hat{\varphi}_1(\hat{\eta})$,are given by homogeneous equations with the solution forced by $\hat{\varphi}_0(\hat{\eta};\ c=0^-)$, $\hat{\varphi}_n(\hat{\eta};\ c=0^+)=-\hat{\varphi}_n(\hat{\eta};\ c=0^-)$, and with boundary conditions readily given by our earlier considerations involving sgn(c). Thus a convenient means for determining the first-order solution for $\hat{\varphi}(\hat{\eta};\ c=0)$ is available.

For the special cases $c=\pm 1$, the second terms in ϵ are, e.g.,

$$\hat{f_1}(\hat{\eta};\ c=1)=\hat{\varphi}_1(\hat{\eta};\ c=1)=\hat{\varphi}_n(\hat{\eta};c=1)$$

Thus the procedures for calculating $\hat{\varphi}_n(\hat{\eta})$ when applied to $c=\pm 1$ yield the ϵ-terms for that case and may be considered to remove the discontinuity in $\hat{f_0}''(\hat{\eta})$, $\bar{\varphi}_0''(\bar{\eta})$ at $\bar{\eta}=\bar{\eta}_0$.

Returning to the more general case of $c\neq 0,\ \pm 1$, we note that nonhomogeneous conditions at $\hat{\eta}\to-\infty$ arise from the matching with $\bar{f}_1(\bar{\eta}_0)$, $\bar{\varphi}_1(\bar{\eta}_0)$ and give λ_2. For most purposes the functions

$$\bar{f}_0(\bar{\eta}),\bar{\varphi}_0(\bar{\eta}),\hat{f_0}(\hat{\eta}),\hat{\varphi}_0(\hat{\eta}),\hat{g}_0(\hat{\eta}),\quad \hat{\varphi}_n(\hat{\eta})$$

give a reasonable approximation to the exact solutions.

Asymptotic Analysis Concluded

From the approximate solutions for a particular c and γ^2, a composite approximation for $f(\eta)$, $\varphi(\eta)$, and $g(\eta)$ can be developed. Since the profiles are usually of most interest, we do so for $f'(\eta)$, $\varphi'(\eta)$, $g(\eta)$ and find

$$f'(\eta)\cong\bar{f}_0'(\bar{\eta}=\eta\epsilon)+\hat{f_0}'(\hat{\eta}=\eta-\bar{\eta}_0/\epsilon-\lambda_1)-\gamma,\quad 0\leq\eta\leq\bar{\eta}_0/\epsilon$$

$$=\hat{f_0}'(\hat{\eta}=\eta-\bar{\eta}_0/\epsilon-\lambda_1),\quad \eta>\bar{\eta}_0/\epsilon$$

$$\varphi'(\eta)=\bar{\varphi}_0'(\bar{\eta}=\eta\epsilon)+\hat{\varphi}_0'(\hat{\eta}=\eta-\bar{\eta}_0/\epsilon-\lambda_1)$$

$$+\epsilon^n\hat{\varphi}_n'(\hat{\eta}=\eta-\bar{\eta}_0/\epsilon-\lambda_1)$$

$$-\mathrm{sgn}(c)\gamma-\epsilon^nB_n(1+n)(\bar{\eta}_0/\epsilon-\eta)^n,\quad 0\leq\eta\leq\bar{\eta}_0/\epsilon$$

$$=\hat{\varphi}_0'(\hat{\eta}=\eta-\bar{\eta}_0/\epsilon-\lambda_1)+\epsilon^n\hat{\varphi}_n'(\hat{\eta}=\eta-\bar{\eta}_0/\epsilon-\lambda_1),\quad \eta>\bar{\eta}_0/\epsilon \qquad (22)$$

These equations apply as they stand for $|n|<1$, i.e., $|c|<1$; for $c=1$, ϵ terms in $\hat{f}(\hat{\eta})$, which have not been included, are comparable to the ϵ^n terms in $\hat{\varphi}(\hat{\eta})$, which have been included. Thus for these special values of c, either the ϵ^n terms in $\varphi'(\eta)$ should be disregarded, or the obvious ϵ^n terms should be added to $f'(\eta)$ so that $f'(\eta)=\varphi'(\eta)$.

The profiles of Eqs. (22) may be used to provide estimates for the integral thicknesses defined by Eqs. (5); in the interest of brevity we do not give the resulting expressions.† We shall present the crucial starting values,

$$\hat{f_0}(0),\bar{\varphi}_0(0),\hat{f_0}(0),\hat{f_0}'(0),\hat{f_0}''(0),\hat{\varphi}_n(0),\text{ etc.},$$

so that a single forward integration will yield the complete solutions.

Remarks on the Numerical Analysis

The numerical analysis of the several sets of equations to be solved in this study involves boundary conditions at two or more points, generally of nonlinear equations. Some of the problems also involve special difficulties such as free boundaries, imposition of particular asymptotic behavior, etc. It is unnecessary to go into the details of our treatment here. The technique of quasilinearization has been employed to obtain linear, first-order equations subject to iteration. The resulting equations have been either treated in difference form, and therefore in terms of matrix iteration, or solved in terms of numerically obtained complementary and particular solutions which are combined so that in each iterate all boundary conditions are satisfied. Generally, careful attention is paid to asymptotic behavior. The techniques used here follow closely those presented in Refs. 9-11.

Results

The results are presented first in terms of the solution to the full equations wherein we extend the previous calculations to

†Interested readers may request from the author an extended report version of this contribution with these and other details.

Table 1 Numerical values for solutions to full equations: $g_w = \gamma^2 = 0.1$, $\sigma = 0.7$

c	$(f+c\varphi)_w$	f''_w	φ''_w	$g'_w/(1-g_w)$	Δ_x	Δ_y	Δ^*	η_0
1	0	0.8381	0.8381	0.6122	0.3090	0.3090	-0.0888	0
	0.5	0.5267	0.5267	0.3786	0.3742	0.3742	-0.0960	0.950
	1	0.2767	0.2767	0.1844	0.4607	0.4607	-0.1053	1.663
	1.5	0.1136	0.1136	0.0502	0.5784	0.5784	-0.1217	2.673
	2	0.0531	0.0531	0.0043	0.7392	0.7392	-0.1647	4.315
	3	0.0333	0.0333	0.0000	1.1221	1.1221	-0.3329	7.894
0.75	0	0.7996	0.7686	0.5730	0.3293	0.3313	-0.0957	0
	0.5	0.4898	0.4592	0.3406	0.4046	0.4062	-0.1043	1.063
	1	0.2460	0.2195	0.1520	0.5079	0.5061	-0.1158	1.895
	1.5	0.0965	0.0780	0.0331	0.6559	0.6400	-0.1388	3.150
	2	0.0510	0.0386	0.0016	0.8645	0.8145	0.2004	5.146
	3	0.0332	0.0250	0.0000	1.3386	1.2106	-0.4018	9.134
0.5	0	0.7595	0.6922	0.5317	0.3541	0.3591	-0.1066	0
	0.5	0.4518	0.3858	0.3012	0.4426	0.4464	-0.1187	1.205
	1	0.2154	0.1601	0.1198	0.5688	0.5612	-0.1363	2.197
	1.5	0.0832	0.0472	0.0187	0.7601	0.7055	-0.1741	3.780
	2	0.0502	0.0254	0.0005	1.0284	0.8751	-0.2660	6.133
	3	0.0333	0.0167	0.0000	1.6098	1.2506	-0.5155	10.580
0.25	0	0.7178	0.6064	0.4883	0.3848	0.3949	-0.1265	0
	0.5	0.4135	0.3049	0.2611	0.4906	0.4979	-0.1480	1.385
	1	0.1869	0.1003	0.0901	0.6476	0.6240	-0.1832	2.582
	1.5	0.0746	0.0219	0.0095	0.8938	0.7499	-0.2581	4.556
	2	0.0498	0.0126	0.002	1.225	0.8712	-0.4011	7.187
	3	0.0334	0.0084	0.0000	1.9122	1.1423	-.7334	12.082
0	0	0.675	0.505	0.423	0.443	0.443	-0.171	0
	0.5	0.379	0.217	0.223	0.550	0.563	-0.224	1.60
	1	0.165	0.042	0.067	0.740	0.674	-0.316	3.01
	1.5	0.071	0.001	0.005	1.027	0.703	-0.485	5.24
	2	0.050	0.000	0.000	1.4	0.71	-0.705	7.95

Table 2 Numerical values from solutions to the inner equations: $g_w = \gamma^2 = 0.1$, $\sigma = 0.7$

c	$\tilde{f}_0(0)$	$\tilde{\varphi}_0(0)$	$\tilde{\eta}_0$	B
-1	-½	-½	3.162	0.0500
0.75	-0.6127	-0.5164	3.598	0.622
0.5	-0.7536	-0.4929	4.115	0.0901
0.25	-0.9098	-0.3608	4.662	0.1667
0	−1	−1	4.97	0.3162

Table 3 Starting values for the outer solutions: $g_w = \gamma^2 = 1.0$, $\sigma = 0.7$

c	$\hat{f}_0(0)$	$\hat{f}'_0(0)$	$\hat{f}''_0(0)$	$\hat{\varphi}_0(0)$	$\hat{\varphi}'_0(0)$	$\hat{\varphi}''_0(0)$	$\hat{g}_0(0)$	$\hat{g}'_0(0)$	$\hat{\varphi}_1(0)$	$\hat{\varphi}'_1(0)$	$\hat{\varphi}''_1(0)$	λ_1
1	0	0.7326	0.2875	0	0.7326	0.2875	0.5924	0.3532	0.2158	-0.0293	0.0744	-1.179
0.75	0.0071	0.7356	0.2661	-0.0094	0.7291	0.2723	0.5924	0.3304	0.2693	-0.0361	0.0784	-1.262
0.5	0.0140	0.7388	0.2433	-0.0281	0.7232	0.2569	0.5922	0.3061	0.3673	-0.0512	0.0897	-1.372
0.25	0.0173	0.7422	0.2191	-0.0692	0.7121	0.2421	0.5917	0.2800	0.5729	-0.0893	0.1123	-1.529
0^+	0	0.7452	0.1938	-0.1800	0.6843	0.2304	0.5902	0.2521	0.7465	-0.1461	0.1067	-1.796
0^-	0	0.7452	0.1938	1.314	0.3922	0.4436	0.5902	0.2521	-0.7465	0.1461	-0.1067	-1.796

large rates in injection. Our principal interest in doing so is to provide a gauge against which the asymptotic solutions can be judged. We then present the results for the inner and outer solutions and compare the predictions of the two analyses.

All the results are for a particular value of the enthalpy ratio $g_w = \gamma^2 = 0.1$ and for a Prandtl number of 0.7, but a range of values of the external flow parameter c and of the injection rate $-(f_w + c\varphi_w)$.

Complete Solutions

In Table 1 we gave the principal results of our solutions of the full equations. Although not directly comparable with the earlier results of Libby,[3] they are fully consistent with them. The main features to be discussed from these tables is that with increasing injection there is a rapid increase in η_0, in the integral thicknesses, and a rapid decrease in the wall-shear and heat-transfer parameters.

We show in Figs. 2a-c the profiles of the two velocity and enthalpy distributions in terms of $f'(\eta)$, $\varphi'(\eta)$, $g(\eta)$ for $c = 0.25$, $-(f_w + c\varphi_w) = 2$. Even for this rate of injection, which must be considered modest in an asymptotic sense, we see evidence of the main features of the boundary layer suggested by the asymptotic analysis for those conditions; specifically a relatively thick inner layer of constant composition, and a thin outer layer. The differences in the behavior of $f''(\eta)$ and $\varphi''(\eta)$ near the outer part of the thick inner reation are also discernable.

Inner Solutions

In Table 2 we give the numerical results for the inner layers, and in Fig. 3 the velocity distributions in terms of $\tilde{f}'_0(\tilde{\eta})$, $\tilde{\varphi}'_0(\tilde{\eta})$; we see the considerably different behavior of the two profiles in general and the unpleasant behavior of $\tilde{\varphi}'(\tilde{\eta})$ near $\tilde{\eta} = \tilde{\eta}_0$ in particular.

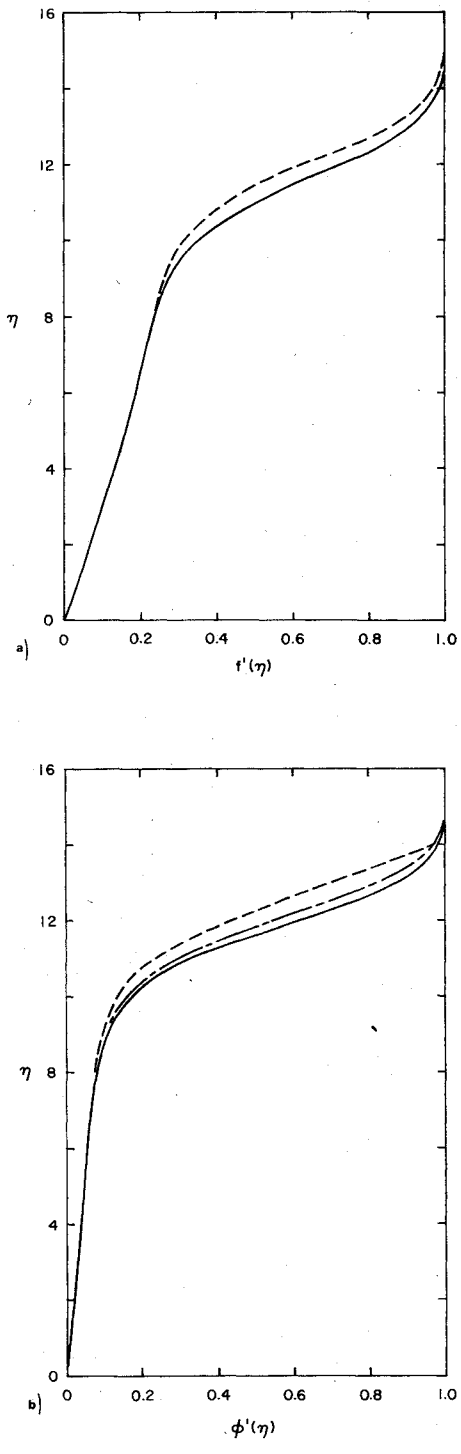

Fig. 2 The profiles for $-(f_w+c\varphi_w)=3$, $c=0.25$. a) The x-wise velocity distribution. Exact solution ——. Asymptotic solution – – –. b) The y-wise velocity distribution. Exact solution ——. Asymptotic solution based on $\tilde{\varphi}_0'(\tilde{\eta})+\hat{\varphi}_0'(\hat{\eta})$ – – –. Asymptotic solution based on $\tilde{\varphi}_0'(\tilde{\eta})+\hat{\varphi}_0'(\hat{\eta})+\epsilon^n\hat{\varphi}_n'(\hat{\eta})$ — – —.

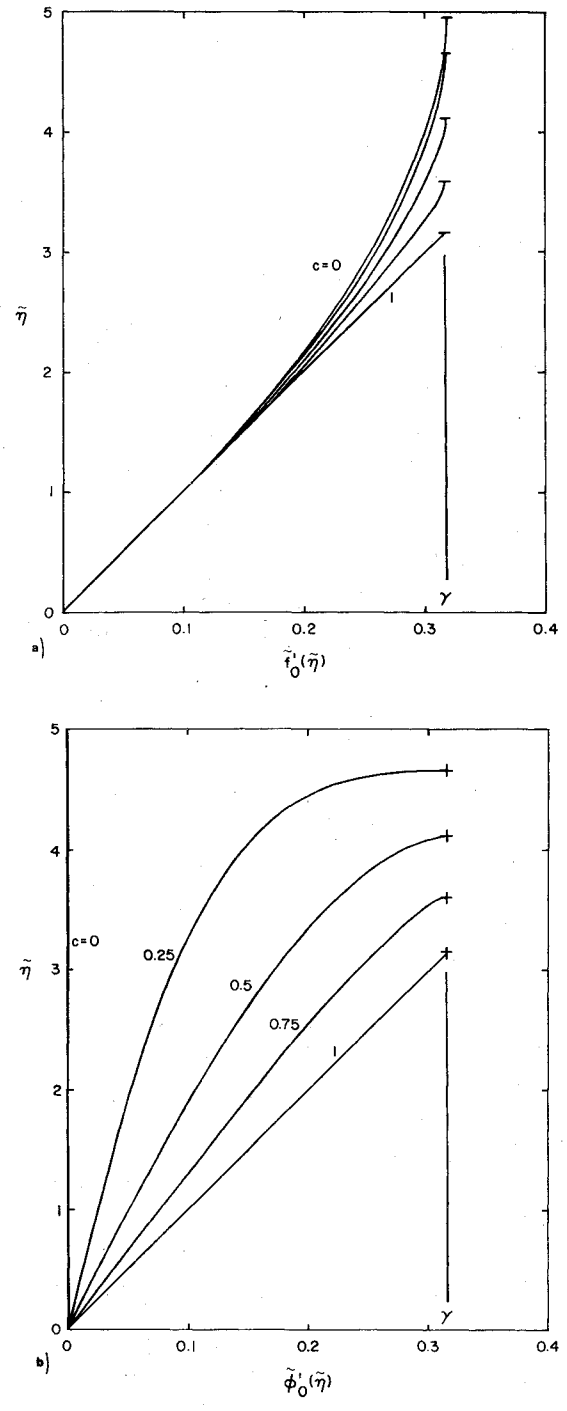

Fig. 3 The velocity profiles for the inner layers. a) The x-wise distribution; b) The y-wise distribution.

Outer Solutions

Table 3 contains the numerical results for the outer solutions in terms of the values at $\hat{\eta}=0$, needed to obtain by forward integration the complete solutions, and of the values of the translation parameter γ_1. Figures 4 shows the outer solution velocity profiles in terms of $\hat{f}_0'(\hat{\eta})$, $\hat{\varphi}_0'(\hat{\eta})$; Fig.5 does this for $\hat{\varphi}_n'(\hat{\eta})$. Of particular interest in Fig. 4b are the different profiles corresponding to $c=0^+$, 0^- with their different asymptotic behavior, $\hat{\varphi}'(\tilde{\eta}\to-\infty)=\gamma$, $-\gamma$, respectively.

Comparison of the Asymptotic and Exact Solutions

Comparison of the predictions of the asymptotic and exact calculations is of interest, and we do so in several ways. On Figs. 2a and 2b we add the results of the asymptotic analysis. In Fig. 2a the x-wise velocity distribution corresponding to the composite solution $\tilde{f}_0'(\tilde{\eta})+\hat{f}_0'(\hat{\eta})$ is compared to the exact solution for $\epsilon=1/3$, $c=0.25$, while in Fig. 2b two comparisons with the exact calculation are possible: with $\tilde{\varphi}_0'(\tilde{\eta})+\hat{\varphi}_0'(\hat{\eta})$ and with the addition of $\epsilon^{0.4}\hat{\varphi}_n'(\hat{\eta})$. Agreement is improved with the additional term, not only in a gross sense but through the removal of the sharp corner corresponding to the infinity in $\tilde{\varphi}_0''(\tilde{\eta}_0)$.

If the various wall values and integral thicknesses as given by the exact and asymptotic solutions are compared, we find that for injection rates corresponding to $\epsilon<1/3$ excellent

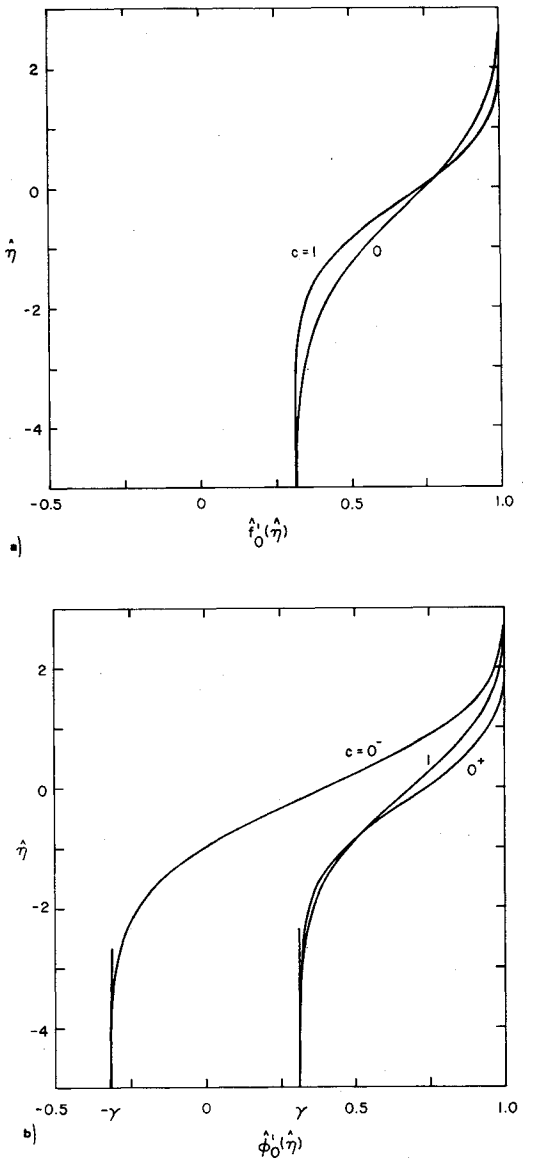

Fig. 4 The velocity profiles for the outer layers. a) The *x*-wise distributions; b) The *y*-wise distributions.

agreement is obtained. With respect to the *y*-wise momentum thickness it is essential to include the $\hat{\varphi}_n(\eta)$ terms. We conclude from this comparison that even for modest rates of injection the asymptotic solutions give a reasonable approximation to the exact calculations.

Conclusions

We have presented a study of the boundary layer at a three-dimensional stagnation point, with special emphasis on large rates of mass transfer. There is found the usual structure of the boundary layer under these conditions, specifically a relatively thick inner layer of constant properties, and a relatively thin outer layer adjusting the inner and external flows. Near the outer edge of the inner layer the velocity distributions in orthogonal directions behave differently, so that the adjustment provided by the outer layer is also different in such directions. It is also found that even if the flow is inward in the outer flow along the *y*-axis, the flow is

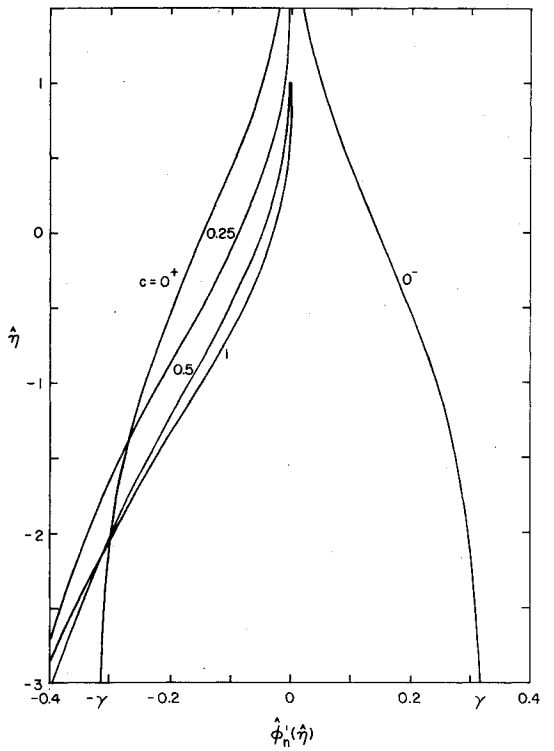

Fig. 5 The second-order *y*-wise velocity profiles in the outer layers.

everywhere outward in the inner layer. Thus significant changes in the outer flow occur in the case of the nearly two-dimensional stagnation point when small outflow changes to small inflow in the external stream.

References

[1] Howarth L., "The Boundary Layer in Three-Dimensional Flow, Part II, The Flow near a Stagnation Point," *Philosophical Magazine*, Vol. 42, 1951, pp. 1,433-1,440.

[2] Davey, A., "Boundary-Layer Flow at a Saddle Point of Attachment," *Journal of Fluid Mechanics*, Vol. 10, 1961, pp. 593-610.

[3] Libby, P. A., "Heat and Mass Transfer as a General Three-Dimensional Stagnation Point," *AIAA Journal*, Vol. 5, March 1967, pp. 507-517.

[4] Kubota, T. and Fernandez, F. L., "Boundary Layer Flows with Large Injection and Heat Transfer," *AIAA Journal*, Vol. 6, Jan. 1968, pp. 22-28.

[5] Kassoy, D. R., "On Laminar Boundary Layer Blow Off," *SIAM Journal of Applied Mathematics*, Vol. 18, Jan. 1970, pp. 29-40.

[6] Libby, P. A. and Kassoy D. R., "Laminar Boundary Layer at an Infinite Swept Stagnation Line with Large Rates of Injection," *AIAA Journal*, Vol. 8, Oct. 1970, pp. 1,846-1,851.

[7] Gersten, K., "Die Kompressible Grenzschichtströmung am Dreidimensionalen Staupunkt bei Starken Absangen oder Ausblasen," *W*ärme-und Stoffubertragung, Vol. 7, 1973, pp. 52-61.

[8] Nachtsheim, P. R. and Green, M. J., "Numerical Solution of Boundary-Layer Flows with Massive Blowing," *AIAA Journal*, Vol. 9, March 1971, pp. 533-535.

[9] Libby, P. A. and Liu, T. M., "Some Similar Laminar Flows Obtained by Quasilinearization," *AIAA Journal*, Vol. 6, August 1968, pp. 1,541-1,548.

[10] Liu, T. M. and Libby, P. A., "Flame Sheet Model for Stagnation Point Flows," *Combustion Science and Technology*, Vol. 2, pp. 377-388.

[11] Wu, P. and Libby, P.A., "Further Results on the Stagnation Point Boundary Layer with Hydrogen injection," *Combustion Science and Technology*, Vol. 6, pp. 159-168.